© 2022. Published by The Company of Biologists Ltd | Biology Open (2022) 11, bio059634. doi:10.1242/bio.059634

RESEARCH ARTICLE

Alpha-T-catenin is expressed in peripheral nerves as a constituent of Schwann cell adherens junctions

Anthea Weng[1,*], Erik E. Rabin[1,*], Annette S. Flozak[1], Sergio E. Chiarella[1,3], Raul Piseaux Aillon[1] and Cara J. Gottardi[1,2,‡]

ABSTRACT

The adherens junction component, alpha-T-catenin (αTcat) is an established contributor to cardiomyocyte junction structure and function, but recent genomic studies link *CTNNA3* polymorphisms to diseases with no clear cardiac underpinning, including asthma, autism and multiple sclerosis, suggesting causal contributions from a different cell-type. We show *Ctnna3* mRNA is highly expressed in peripheral nerves (e.g. vagus and sciatic), where αTcat protein enriches at paranodes and myelin incisure adherens junctions of Schwann cells. We validate αTcat immunodetection specificity using a new *Ctnna3*-knock-out fluorescence reporter mouse line yet find no obvious Schwann cell loss-of-function morphology at the light microscopic level. *CTNNA3*/*Ctnna3* mRNA is also abundantly detected in oligodendrocytes of the central nervous system via public databases, supporting a general role for αTcat in these unique cell–cell junctions. These data suggest that the wide range of diseases linked to *CTNNA3* may be through its role in maintaining neuroglial functions of central and peripheral nervous systems.

This article has a corresponding First Person interview with the co-first authors of the paper.

KEY WORDS: Schwann cell, Catenin, Myelination, Neuroglia, Peripheral nerve, Vagus

INTRODUCTION

Alpha-catenins are a family of adherens junction proteins that organize individual cells into tissues through an ability to tether the cadherin/β-catenin cell–cell adhesive complex to actin filaments. They are encoded by separate genes and historically named according to tissue-types where first identified: αE^{pithelial}-catenin/*CTNNA1*, αN^{eural}-catenin/*CTNNA2*, αT^{estes}-catenin/*CTNNA3* (Chiarella et al., 2018). αEcat (*CTNNA1*) is now appreciated as broadly expressed and essential for the development and homeostasis of most tissue types (Janssens et al., 2001), leading to it being the most studied form of α-catenin (Herrenknecht et al., 1991; Hirano et al., 1992; Torres et al., 1997; Lien et al., 2006; Vasioukhin et al., 2001; Sheikh et al., 2006). αNcat (*CTNNA2*) expression is largely restricted to the brain, where it plays critical roles in neuronal synapses required for full brain development (Park et al., 2002; Uemura and Takeichi, 2006). αT-cat (*CTNNA3*) is the most recently evolved α-catenin, but in contrast to its ancestral relatives (αE-cat and αN-cat) appears developmentally dispensable, as *Ctnna3* knock-out mice are viable and fertile (Li et al., 2012; Vite et al., 2015). Despite its name, αTcat is best known for its role in the heart (Vite et al., 2015), where it contributes to the interspersed alignment of adherens junctions and desmosomes at the intercalated disk of cardiomyocytes (Janssens et al., 2003; Franke et al., 2006; Li and Radice, 2010; Li et al., 2019). This organization is critical for long-term cardiac function, since *Ctnna3* knock-out mice develop age-related cardiomyopathy, similar to patients with loss-of-function mutations in αTcat (Janssens et al., 2003; van Hengel et al., 2013). These data have led to the notion that αT-cat plays an important but highly restrictive role in cardiomyocyte functionality.

Curiously, recent genetic association studies have linked mutations, non-coding polymorphisms and copy number variants (CNV) in *CTNNA3* to a wide spectrum of diseases, including asthma, (Kim et al., 2009; Bernstein et al., 2013; McGeachie et al., 2015; Perin and Potocnik, 2014), food allergy (Li et al., 2015), autism spectrum disorder (Wang et al., 2009; O'Roak et al., 2012; Bacchelli et al., 2014), multiple sclerosis (Vilarino-Guell et al., 2019), diabetes (Zhang et al., 2021) and Alzheimer's (Smith et al., 2006; Miyashita et al., 2007). These disease associations are challenging to rationalize in context of the supposed restricted expression of αT-cat to cardiomyocytes and testes, suggesting αT-cat /CTNNA3 disease linkages may occur via an unappreciated cell/tissue-type. Moreover, while some of the aforementioned genetic studies show genotype/mRNA abundance phenotype correlations (Kim et al., 2009; McGeachie et al., 2015), far fewer show causal changes at the αT-cat protein level, where cross-reactivity of commercially available antibodies between α-catenin family members has been problematic.

Our group previously validated αT-cat's linkage to steroid-resistant asthma using the house-dust mite model, where *Ctnna3* knock-out mice showed greatly attenuated airway hyperreactivity (Folmsbee et al., 2016a). Despite our observing cardiomyocytes of pulmonary veins as the major αT-cat-expressing cell in lung (Folmsbee et al., 2015; Folmsbee and Gottardi, 2017), the cell type through which αT-cat loss leads to reduced airway hyperreactivity has remained elusive. Here, we show that αT-cat protein is abundantly expressed in peripheral nerves (e.g. vagus and sciatic), specifically within the Schwann cell component. Since nerves innervate most organ systems and tissue types, we reason that many αT-cat /*CTNNA3* disease linkages should be considered via its role in neuroglial cell types.

[1]Department of Pulmonary Medicine, Northwestern University, Feinberg School of Medicine, Chicago, IL 60611, USA. [2]Cell & Developmental Biology, Northwestern University, Feinberg School of Medicine, Chicago, IL 60611, USA. [3]Mayo Clinic, Rochester, MN 55902, USA.
*Co-first authorship

‡Author for correspondence (c-gottardi@northwestern.edu)

A.W., 0000-0003-3909-8861; E.E.R., 0000-0002-8967-6482; S.E.C., 0000-0002-0445-4929; C.J.G., 0000-0003-0912-7617

Received 20 September 2022; Accepted 16 November 2022

Biology Open (2022) 11, bio059634. doi:10.1242/bio.059634

RESULTS

Early work on αT-cat/*CTNNA3* used a human cDNA Rapid-Scan™ panel to identify heart and testis as major tissue-types expressing *CTNNA3*, although low levels of RNA were also detected in brain, kidney and liver (Janssens et al., 2001). To better assess the full range of cell- and tissue-types expressing αT-cat /*CTNNA3*, we interrogated the Genotype-Tissue Expression (GTEx)-database, an NIH Common Fund resource to study relationships between genetic variation and gene expression across multiple reference tissues (GTEx Consortium, 2013). This database also serves as a convenient resource to validate RNA abundance across a greater range of tissues (~50-types), especially those not typically harvested in earlier studies (e.g. nerve, sub-regions of brain). This tissue-wide bulk-RNA sequencing database reveals *CTNNA3* expression in tibial nerve, spinal cord and various brain regions (substantia nigra, hippocampus, amygdala) at levels comparable to those observed in heart and testes (https://gtexportal.org/home/gene/CTNNA3). Additionally, single-cell expression within this database reveals *CTNNA3* enrichment in the Schwann cell component of multiple tissues including skeletal muscle, esophagus, prostate and heart. Thus, the GTEx resource reveals that in addition to established expression of in myocytes, *CTNNA3* is also abundantly expressed in the glial component of peripheral nerve.

Since spinal cord and brain register the highest *CTNNA3* expression levels across human tissues, we sought to determine whether this expression might be through a related glial cell-type. To interrogate *CTNNA3* expression in both central and peripheral nervous system, we examined more sensitive RNA-sequencing datasets from enriched (i.e. flow-sorted) cell populations. The Barres Lab RNA-sequencing dataset analyzed gene expression in the cells from the central nervous system, revealing abundant *CTNNA3/Ctnna3* expression in oligodendrocytes and their precursor cells in both humans and mice (Zhang et al., 2014, 2016). Additionally, the Sciatic Nerve Atlas (SNAT) examined peripheral nerve cell types within mouse sciatic nerve, showing prominent *Ctnna3* expression in Schwann cells (Gerber et al., 2021). Since oligodendrocytes and Schwann cells use cytoplasmic myelin to sheath and thereby insulate neurons of both central and peripheral nervous systems respectively, these databases suggest that αT-cat may support a common role in these functionally related cell types.

Generation and characterization of a novel Ctnna3-fluorescent reporter mouse

In an attempt to visualize αT-cat expression in cell- and tissue-types not optimally captured by typical paraffin-embedded thin-section methods, we generated a fluorescent reporter mouse in collaboration with Northwestern University's Transgenic Mouse Core. Using CRISPR-Cas9 gene editing, a membrane anchored enhanced green fluorescent protein (eGFPcaax) (Hines et al., 2015) was knocked into exon 2 of the *Ctnna3* gene. The *Ctnna3* promoter drives GFP expression while simultaneously knocking out native expression of αT-cat/*Ctnna3* (Fig. 1A). We analyzed eGFPcaax-reporter expression in tissues known to express αTcat protein: heart and testes. We confirmed GFP protein expression in heart tissue from heterozygous (*Ctnna3*$^{GFP/+}$), but not wild-type (*Ctnna3*^{WT}) mice by immunoblot analysis (Fig. 1B). As expected, *Ctnna3*$^{GFP/+}$ and *Ctnna3*$^{KO\ (GFP/GFP)}$ mice showed allele-dependent loss of αT-cat protein with complementary changes in GFP abundance in both heart and testes (Fig. S1A). No GFP is detected in tissues lacking *Ctnna3* expression, such as liver or kidney (Fig. S1B). While GFP expression from this *Ctnna3*$^{GFP/+}$ reporter was sufficiently abundant to detect by immunoblotting (Fig. 1B), we were unable to detect GFP by immunofluorescence analysis with an anti-GFP antibody previously validated by our group for use on paraffin-embedded or whole mount samples, even in *Ctnna3*$^{KO(GFP/GFP)}$ with two copies of GFP (Fig. 1C; GFP staining not shown). Although our GFP reporter contains a membrane-targeting lipid modifiable -CAAX motif to improve membrane enrichment (Hines et al., 2015), we reason the ability of αTcat to enrich at cadherin/β-cat junctions improves its detection in comparison with the GFP-caax, which

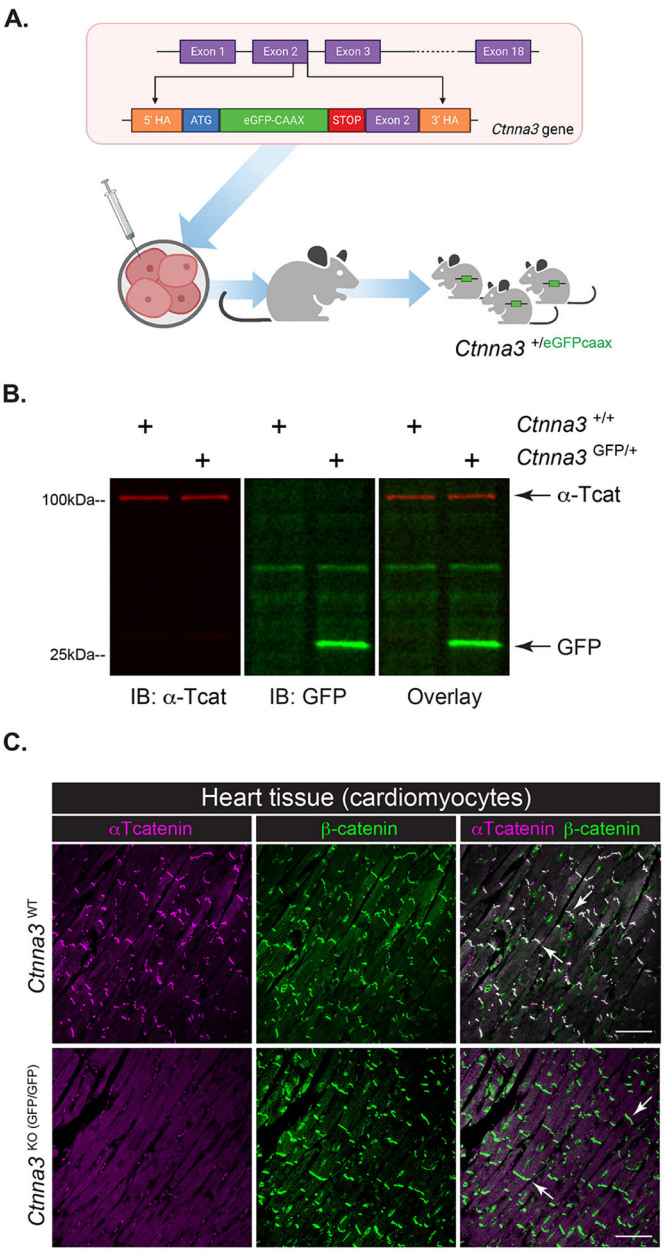

Fig. 1. Generation and characterization of a novel fluorescent *Ctnna3*-reporter mouse. (A) Reporter design schematic by BioRender. Membrane-anchored eGFPcaax was inserted into exon 2 of the *Ctnna3* gene. Construct was nucleofected into embryonic stem cells, clones with correct construct insertion were selected, and two chimeric males were generated. (B) Immunoblotting of *Ctnna3*^{WT} and *Ctnna3*$^{GFP/+}$ heart lysates with anti-αTcat (red) and anti-GFP (green) antibodies. (C) Representative images of heart sections from *Ctnna3*^{WT} and *Ctnna3*$^{KO\ (GFP/GFP)}$ mice. Scale bars: 50 µm. Immunofluorescence staining of cardiomyocytes by β-catenin (β-cat; green) and αTcat (magenta). Arrows indicate intercalated disk-type adherens junctions in cardiomyocytes.

Biology Open (2022) 11, bio059634. doi:10.1242/bio.059634

distributes across various membrane compartments in the cell. Nonetheless, these data show we have generated a GFP-reporter mouse for *Ctnna3* expression (*Ctnna3*$^{GFP/+}$) that also effectively deletes the endogenous αT-cat protein when crossed to homozygosity (*Ctnna3*$^{KO\ (GFP/GFP)}$).

αTcat/*Ctnna3* is expressed in vagus nerve

A number of genome-wide association studies have linked *CTNNA3* to chemical-induced occupational asthma (Kim et al., 2009; Bernstein et al., 2013), steroid refractory asthma (Perin and Potocnik, 2014) and asthmatic exacerbations (McGeachie et al., 2015). Indeed, our team validated αT-cat's linkage to asthma using the house-dust mite model, where *Ctnna3* knock-out mice showed greatly attenuated airway hyperreactivity (Folmsbee et al., 2016a). However, despite our observing cardiomyocytes of pulmonary veins as the major αT-cat-expressing cell in lung (Folmsbee et al., 2016a, 2015; Folmsbee and Gottardi, 2017), the cell type through which αT-cat loss leads to reduced airway hyperreactivity has remained elusive. Given evidence via the GTEx database that *CTNNA3* is abundantly expressed in peripheral nerves, where parasympathetic peripheral nerve inputs are known to innervate airways and control smooth muscle contractility/reactivity responses (Lewis et al., 2006; McGovern and Mazzone, 2014; McAlexander et al., 2015), we sought to determine whether αTcat protein might be expressed in the vagus. We harvested small (~0.5 cm) segments of the vagus nerve and nodose ganglion just anterior to the thoracic cavity of wild-type (*Ctnna3*^{WT}) and knock-out (*Ctnna3*$^{KO\ (GFP/GFP)}$) mice for total protein and RNA extraction (Fig. 2A, schematic). We confirmed αTcat expression in both nodose ganglion and vagus nerve in wild-type mice; knock-out tissue showed no αTcat (Fig. 2B). Remarkably, we detected *Ctnna3* RNA expression in vagus and nodose at levels comparable to and even greater than *Ctnna3* levels in heart (Fig. 2C). The lack of correlation between *Ctnna3* RNA and protein abundance raises the possibility that tissues may differentially regulate αTcat at the protein level. Moreover, since αTcat/*Ctnna3* RNA is as abundant in vagus segments as in nodose ganglion, where the latter contains neuronal cell bodies, we reason that the bulk of *Ctnna3* signal may be due to its expression in Schwann cells, consistent with database resources showing little *Ctnna3* RNA in neurons (Zhang et al., 2014, 2016).

αTcat is expressed along Schwann cell myelin incisures of sciatic nerve

To specifically address whether αTcat protein is expressed in the Schwann cell component of peripheral nerves, we turned to the sciatic nerve due to its large size and ease of dissection (Fig. 3A, Movie 1). We validated αTcat protein expression in sciatic nerve lysates harvested from *Ctnna3*^{WT} but not *Ctnna3*$^{KO\ (GFP/GFP)}$ mice; the ubiquitous αEcat protein remained largely unchanged (Fig. 3B). Immunofluorescence staining of wild-type sciatic nerve revealed αTcat localization to paranodal regions of glial-axon junctions, as well as structures reminiscent of myelin incisures, thin regions of Schwann cell cytoplasm excluded from compact myelin regions (Fig. 3C). Also known as Schmidt-Lanterman incisures, this structure results from successive concentric wraps of Schwann cell cytoplasm around an axon, where each wrapping is held together by adherens junction proteins in a uniquely characteristic intracellular 'autotypic' junction (Fannon et al., 1995; Tricaud et al., 2005). As expected, αTcat protein co-localizes with known adherens junction markers, E-cadherin and F-actin (Fig. 4). Importantly, *Ctnna3*$^{KO\ (GFP/GFP)}$ mice showed no detectable αTcat immunostaining (Fig. 3C, bottom and 3D, right). We observed no obvious structural defect in these nerves, as overall E-cadherin and F-actin staining patterns were similar. Disappointingly, we were also unable to rely on GFP immunostaining as a convenient reporter for *Ctnna3* expression in this tissue, even in *Ctnna3*$^{KO\ (GFP/GFP)}$ mice with two copies of eGFPcaax (not shown). In summary, these data show that αTcat protein localizes to Schwann cell autotypic and heterotypic junction structures with familiar partners, E-cadherin and F-actin.

DISCUSSION

αTcat is the most recently evolved member of the alpha catenin family and best known for its role in cardiomyocyte junctions of heart, where its loss leads to an age-related cardiomyopathy that phenocopies disease in patients with αTcat loss-of-function mutations (Vite et al., 2015). These data have led to the notion that αT-cat plays an important but highly restrictive role in cardiomyocyte functionality. However, numerous genetic association studies have linked *CTNNA3* to a wide spectrum of diseases, ranging from asthma and food allergy to autism, multiple

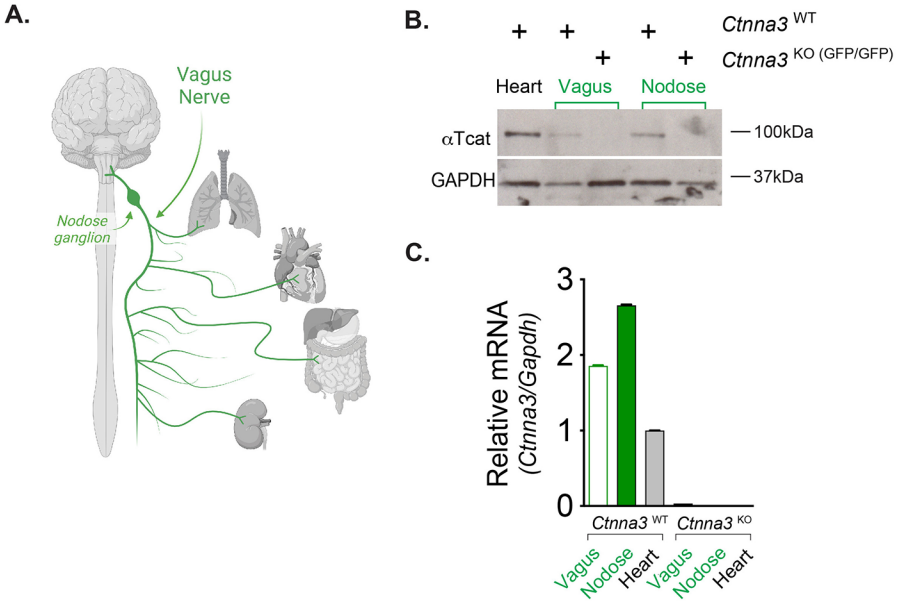

Fig. 2. αTcat is expressed in vagus nerve. (A) Schematic of nodose ganglion, vagus nerve and organs innervated by vagus (Biorender). (B) Western blot of *Ctnna3*^{WT} and *Ctnna3*$^{KO\ (GFP/GFP)}$ heart, vagus and nodose tissue with anti-αTcat and loading control GAPDH. (C) mRNA relative expression via real-time quantitative PCR analysis of *Ctnna3*^{WT} and *Ctnna3*$^{KO\ (GFP/GFP)}$ RNA isolated from heart, vagus and nodose tissues. Error bars reflect technical (n=3) rather than biological replicates due to difficulty harvesting tissue and independent validation of αTcat protein in B.

Biology Open (2022) 11, bio059634. doi:10.1242/bio.059634

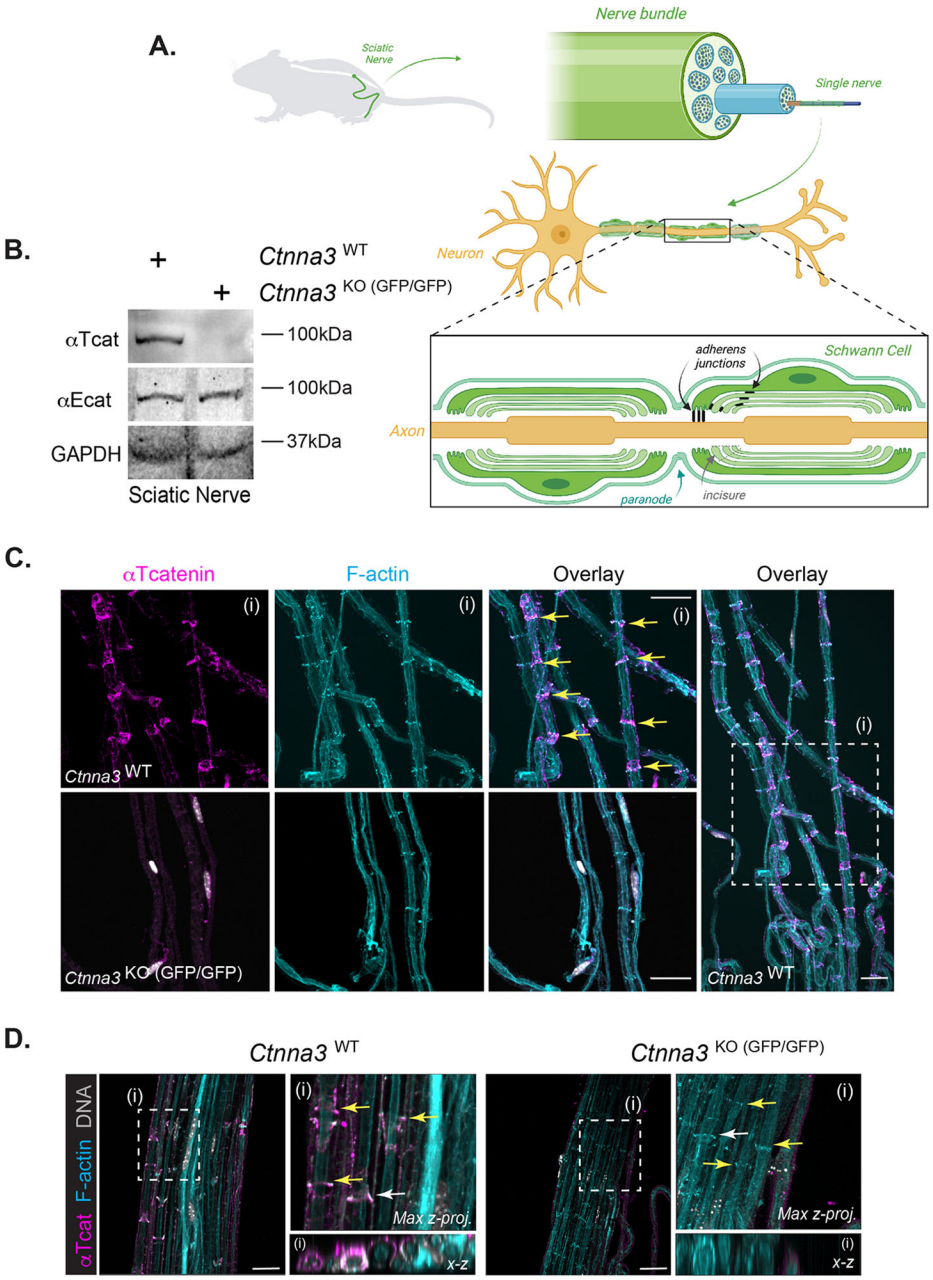

Fig. 3. αTcat is expressed at myelin incisure and paranodal loop regions of Schwann cells in sciatic nerve. (A) Schematic (Biorender) demonstrating αTcat expression at adherens junctions along myelin incisures and paranodal loops of Schwann cells from sciatic nerve. (B) Western blot of *Ctnna3*^{WT} and *Ctnna3*$^{KO\ (GFP/GFP)}$ sciatic nerve tissue with anti-αTcat, anti-αEcat, and loading control GAPDH. (C,D) Representative confocal images of sciatic nerve sections from adult (8-12 weeks) from *Ctnna3*^{WT} and *Ctnna3*$^{KO\ (GFP/GFP)}$ mice; one field of view from low- and high-magnification inset (boxed region) are shown (box i). Low-magnification view for Ctnna3$^{KO\ (GFP/GFP)}$ is not shown. Immunofluorescence staining of myelin incisures by αTcat (magenta) and F-actin (cyan). DNA labeling by Hoechst (gray). Scale bars: 25 µm. Yellow arrows indicate adherens junctions where αTcat co-localizes with F-actin. (D) Maximum intensity z-projection images were generated with Imaris from confocal images. White arrows indicate plane of x-z section.

sclerosis, diabetes and Alzheimer's (Kim et al., 2009; Bernstein et al., 2013; McGeachie et al., 2015; Perin and Potocnik, 2014; Li et al., 2015; Wang et al., 2009; O'Roak et al., 2012; Bacchelli et al., 2014; Vilarino-Guell et al., 2019; Zhang et al., 2021; Smith et al., 2006; Miyashita et al., 2007). These disease associations have been puzzling to rationalize in context of established restricted expression of αT-cat to cardiomyocytes (or testes), suggesting αT-cat/*CTNNA3* disease linkages may occur via an unappreciated cell/tissue-type. Guided by the human tissue gene expression (GTEx) database, we demonstrate αTcat protein is also highly expressed in peripheral nerves (e.g. vagus and sciatic), specifically within the Schwann cell component. *CTNNA3/Ctnna3* mRNA is also abundantly expressed in oligodendrocytes of the central nervous system (Zhang et al., 2014, 2016). Together with previous evidence that αTcat localizes to apical junctions of ependymal cells (Folmsbee et al., 2016b), we propose a generalized role for αT-cat in neuroglial functions. Since neuroglia participate in central and peripheral nervous systems, where the latter innervate all organs of the body, we speculate that the wide range of αT-cat/*CTNNA3* disease linkages may be considered via its role in neuroglial cell types.

Anticipating the need to visualize *Ctnna3* gene expression in a cell type challenging to resolve by thin section imaging (e.g. Schwann cells), we generated a novel fluorescent reporter *Ctnna3*$^{GFP/+}$ knock-out mouse. While we validated this reporter line for GFP expression and consequent loss of αTcat, we were unable to visualize the membrane-anchored GFP reporter by immunofluorescence analysis. Whether this is due to sequences in *Ctnna3* that enhance the translation efficiency of αTcat, or the ability of αTcat to become highly enriched at cell–cell junctions compared with a general membrane-localized GFP is not clear. Nonetheless, this reporter may ultimately prove valuable for future studies seeking to characterize consequences of *Ctnna3*/αTcat loss in neuroglial cell types.

Biology Open (2022) 11, bio059634. doi:10.1242/bio.059634

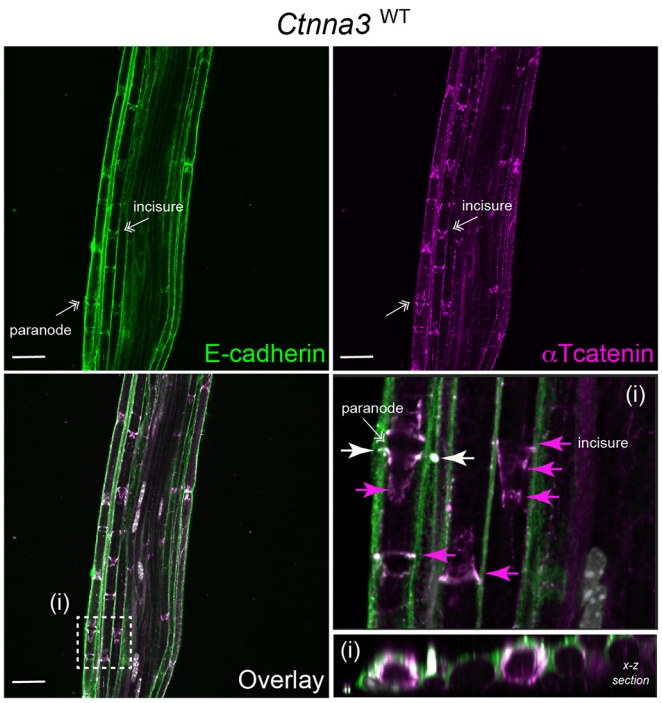

Fig. 4. *Ctnna3* co-localizes with known junction marker, E-cadherin. Representative confocal images of sciatic nerve sections from adult (8-12 weeks) wild-type (*Ctnna3*^{WT}) reporter mice; one field of view from low- and high-magnification insets (boxed region) are shown (box i). Immunofluorescence staining of adherens junction in myelin incisures by E-cadherin (green) and αTcat (magenta). DNA labeling by Hoechst (gray). Scale bars: 25 µm. White arrows indicate plane of x-z section. Areas of E-cadherin and αTcat co-localization are revealed by white fluorescent staining, showing αTcat co-localizes with known junction markers at myelin incisures in sciatic nerve.

It is intriguing that αTcat/*CTNNA3* expression is restricted to Schwann cells of peripheral nerves and oligodendrocytes in brain, two cell-types known to play critical roles in the myelination and insulation of neurons. Our evidence that αTcat specifically localizes to paranodes and myelin incisures of Schwann cells was not entirely surprising, given previous evidence that both structures comprise modified adherens junctions enriched for cadherins and catenin proteins (Fannon et al., 1995; Tricaud et al., 2005). Paranodes reflect regions of heterotypic glial cell-axon contact, whereas Schmidt-Lanterman myelin incisures reflect an alignment of successive wraps of Schwann cell cytoplasm around an axon, where each wrap is held together by adherens junction proteins (Fannon et al., 1995). While forced-expression of dominant-inhibitory versions of cadherin-catenin complex components can perturb this structure (Tricaud et al., 2005), whether polymorphisms or mutation in members of this cadherin-catenin adhesive complex can alter the critical function of Schwann cells (and related oligodendrocytes) relevant to disease remains unknown.

Our evidence that αTcat protein is detected in the vagus, which innervates the majority of visceral tissues throughout the body, offers an attractive lens through which we may view genetic linkages between αTcat/*CTNNA3* and a range of diseases (reviewed in (Chiarella et al., 2018). With regards to *CTNNA3* linkages to steroid-resistant asthma, our team previously validated this association showing that *Ctnna3*^{KO} mice display reduced airway hyperreactivity in response to methacholine challenge. Our evidence that αTcat is expressed in the vagus, a known regulator of airway smooth muscle responses (Lewis et al., 2006; McGovern and Mazzone, 2014; McAlexander et al., 2015), suggests the intriguing possibility that αTcat/*CTNNA3* contributes to asthmatic airway responses through its role in the Schwann cell-myelinating component of peripheral nerves. Indeed, even *CTNNA3*'s linkages to heart disease merit revisiting, where recent linkages to atrial fibrillation/Brugada Syndrome (Maltese et al., 2019) may be due to a peripheral nerve rather than a cardiomyocyte junction defect (Teodorovich et al., 2016).

METHODS

Ctnna3 membrane-anchored GFP reporter mouse

We knocked-in a membrane associated eGFP construct into exon2 of the *Ctnna3* locus using CRISPR gene editing in collaboration with Northwestern's Transgenic and Targeted Mutagenesis Laboratory. By design, the *Ctnna3* promoter drives eGFP-caax expression from the endogenous locus, while knocking out expression of the gene. Note, addition of an exogenous bGH polyA immediately downstream of the stop codon was required to improve eGFP-caax expression from the endogenous *Ctnna3* exon 2 locus, given the extremely large size of the *Ctnna3* gene. We nucleofected the following into murine B6N-derived embryonic stem (ES) cells: *Ctnna3*-targeting CRISPR reagents, an eGFP repair plasmid designed to insert into the *Ctnna3* exon2 locus, and a non-targeting PGK-plasmid harboring a puromycin selection cassette. Puromycin resistant ES cell clones were selected, propagated and genotyped for correct construct insertion. Targeted clones were expanded and validated, with select clones injected into albino B6J blastocyst stage embryos. Briefly, donor females (albino B6J) are hormone treated, mated, and plugged. Recipient (foster) females are also set up. ES cells are injected into the cavity of an expanded blastocyst stage embryo and injected embryos are surgically transferred into the reproductive tract of recipient females to generate chimeric mice. Chimeric mice were genotyped for correct insertion of the construct into the *Ctnna3* locus. Two chimeric males (90% and 95%) were generated and bred to C57BL/6J mice, transmitting GFP to the F1 generation with initial genotype validation by endpoint PCR and currently via real-time PCR with Transnetyx (Cordova, TN). GFP expression was validated by immunoblot/immunostaining analysis of target tissues. Detailed mouse report with PCR-gel validation will be provided upon request. This line will be available at Jax labs (stock number 037394) under the name C57BL/6-Ctnna3em1Cgot. All experimental protocols were approved by the Institutional Animal Care and Use Committee at Northwestern University.

Tissue collection

Mice were euthanized and perfused with 10 ml of HBSS. For heart dissection, tissue was fixed in 4% PFA overnight at 4°C, then transferred into 70% ethanol for dehydration, paraffin embedding and ∼4 µm sectioning via microtome. For vagus nerve and nodose ganglion dissection, skin, salivary glands, and masticatory muscles were removed, followed by identification of the trachea, carotid artery, and glossopharyngeal nerve. The vagus nerve and nodose ganglion were identified, excised, and stored at −20°C for further processing as previously described (Norgren and Smith, 1994). For sciatic nerve dissection, skin and muscle of upper hind legs were removed, and a ∼3 mm segment of sciatic nerve was cut and placed into Zamboni's fixative for 10 min, followed by 15% glycerol/PBS solution (v/v) for 24 h at 4°C. Nerves were then incubated in successive glycerol solutions (45%, 60%, 66% glycerol in PBS) for 18-24 h each at 4°C. Tissue was stored at −20°C until ready for further processing. Nerve bundles were further dissected into individual fibers using a Leica MZFLIII dissecting microscope. Briefly, nerves were placed into 10 cm dishes containing HBSS. Nerves were teased apart using 30G needles and individual fibers were placed onto poly-L-lysine-coated Bond380 slides. Slides were then dried and stored at −20°C.

Immunofluorescent staining and imaging

For paraffin-embedded heart slides: Slides were de-paraffinized by submerging in xylene twice for 5 min each. Slides were then gradually rehydrated in 100%, 90%, and 70% EtOH solutions twice for 2 min

Biology Open (2022) 11, bio059634. doi:10.1242/bio.059634

followed by three washes in PBS for 5 min each. Slides were subsequently quenched in a 10 mM glycine solution for 15 min at room temperature. Slides were simmered in a citrate-based antigen retrieval buffer for 30 min at 95°C. After cooling to 25°C, slides were briefly rinsed in PBS before immunostaining. For heart and sciatic nerve tissue, slides were blocked in a solution of 10% normal goat serum (NGS) in 0.3% TritonX-100 PBS for 30 min at 25°C. Slides received primary antibody prepared in a solution containing 3% NGS in 0.3%TritonX-100 PBS and incubated for 1 h at 25°C. Following primary antibody, slides were rinsed in PBS and then incubated in fluorescence conjugated secondary antibody for 30 min at 25°C. Tissue sections were briefly rinsed in water and mounted using ProLong Gold anti-fade mounting media. Heart tissue was imaged on a Zeiss Axioplan2 epifluorescence microscope. Sciatic nerves were imaged at Northwestern University's Center for Advanced Microscopy core using a Nikon W1 spinning disk confocal microscope. 20× z-stack images were taken in 0.5 µm steps whereas 60× *z*-stack images were taken in 0.25 µm step sizes. All image files were pseudo-colored in FIJI for presentation in figures. Three-dimensional (3D) imaging of sciatic nerve was analyzed using Imaris software. Orthogonal views were obtained from maximum intensity projection (MIP) images. Videos were created via 3D reconstruction of z-stacks (10-25 µm depth; 0.25 µm step size).

Tissue preparation and Western blotting

Heart, vagus/sciatic nerve and nodose ganglion tissues were collected and snap-frozen in liquid nitrogen. Heart tissue was homogenized on ice using Tissue Tearor at medium speed for 1 min in lysis buffer (RIPA plus 0.1% SDS with Roche EDTA-free protease inhibitor) and allowed to sit on ice 10 min followed by sonication using Branson sonifier at 10% amplitude, 1 s on/off intervals for 10 rounds total. Lysates were centrifuged at 14,000 ***g*** for 10 min at 4°C and the supernatant collected and stored at −80°C. Vagus nerve and nodose tissues were processed as described except that tissues were pipetted up and down 20 times in lysis buffer using a large bore tip and allowed to sit on ice 10 min before sonication and centrifugation. Protein concentrations were determined via Bradford assay. Samples were diluted in 2× SDS loading buffer and boiled at 95°C for 5 min prior to loading. 50 µg of protein was run on a 4-20% gel at 120 V for 90 min. Following gel transfer, nitrocellulose membranes were rinsed in Ponceau S to confirm presence of protein. Membranes were blocked for 1 h at room temperature in 5% milk/TBS-T, followed by incubation in primary antibody in 5% BSA/TBS-T overnight with rocking at 4°C. After primary antibody incubation, membranes were washed three times for 10 min in TBS-T. Membranes received secondary antibody (HRP or fluorescent conjugated) prepared in a 5% milk/TBS-T solution for 1 h at room temperature with rocking. Membranes were then washed three times for 15 min in TBS-T before either incubation with Pierce ECL Plus solution for 1 min or direct fluorescence imaging on Licor Odyssey Fc scanner for 2-10 min.

RNA isolation and PCR analysis

RNA was extracted from snap-frozen heart, vagus nerve, and nodose ganglion tissue using the Qiagen RNeasy Plus Mini Kit as per manufacturer instructions. Briefly, tissue samples were lysed in 600 ml RLT buffer using sterile Beadbug homogenization tubes with 3 mm ceramic beads and Benchmark Beadblaster shaker run at power setting 4, 30 s shake with 30 s intervals, for four cycles and repeated the program twice. Homogenized sample was centrifuged at 14,000 ***g*** for 3 min. Supernatant was applied to Qiagen gDNA Eliminator spin columns before continuing with Qiagen protocol. RNA was eluted in 40 ml nuclease-free water. First strand cDNA was reverse transcribed from equal amounts of total RNA using iScript cDNA synthesis kit (Biorad, Hercules, CA, USA). Specific primers for amplification of the mouse *Ctnna3* message: forward primer (FP) 5'-GGTTACTACCCTGGTGAATTGTCC-3′, reverse primer (RP) 5'-CTCTTTTCGAACTTCCTGGAGTGC-3′. Real-time PCR was performed using iQ SYBR Green Supermix according to the manufacturer instructions (Biorad, Hercules, CA, USA). PCR was carried out in 96-tube plates using the MyiQ Single Color Real-Time PCR Detection System and software (Bio-Rad). All reactions were done in triplicate with negative controls. Gapdh was used as the internal control. The relative change in gene expression was calculated using the $2^{\Delta\Delta Ct}$ method.

KEY RESOURCES

Reagent or resource	Source	Identifier
Antibodies		
Anti-alpha-T-catenin (rat monoclonal) (immunofluorescence)	VanRoy lab, University of Ghent, Belgium Jolanda.VanHengel@UGent.be	1159_12A4S4; recognizes human/mouse; raised against MLAPKEDRLNANKNI; Janssens et al., 2001
Anti-alpha-T-catenin (rabbit polyclonal) (immunoblotting)	VanRoy lab, University of Ghent, Belgium Jolanda.VanHengel@UGent.be	Anti-peptide Ab #942; Raised against KIHPLQVMSEFRGRQIY of human αT-cat Janssens et al., 2001
Anti-E-cadherin	BD Biosciences	Catalogue number 610182
Anti-GAPDH	EMD-Millipore	Catalogue number CB1001
Anti-GAPDH	Santa Cruz	Catalogue number SC-25778
Anti-GFP	Invitrogen	Catalogue number A11122
Anti-alpha-E-catenin	Enzo	Catalogue number ALX-804-101
Alexa Fluor 680 Phalloidin	Invitrogen	Catalogue number A22286
Goat anti-rabbit Alexa Fluor 568	Invitrogen	Catalogue number A11001
Goat anti-rat Alexa Fluor 594	Invitrogen	Catalogue number A11007
Goat anti-mouse Alexa Fluor 488	Invitrogen	Catalogue number A28175
Donkey anti-mouse IRDye 680RD or 800CW	Li-Cor	Catalogue number 926-68073, 926-32213
Donkey anti-rabbit IRDye 680RD or 800CW	Li-Cor	Catalogue number 926-68072, 926-32212
Goat anti-rabbit IgG (H+L)-HRP	Bio-Rad	Catalogue number 1706515
Goat anti-rat IgG-HRP	Millipore	Catalogue number AP136P
Kits		
RNAeasy Plus Mini RNA isolation kit	Qiagen	Catalogue number 74134
Criterion 4-20% TGX acrylamide gel	Bio-Rad	Catalogue number 5671093 or 5671094
Transblot Turbo Transfer Pack Midi 0.2um nitrocellulose	Bio-Rad	Catalogue number 1704159
Protein Assay Dye Concentrate	Bio-Rad	Catalogue number 5000006
ECL2 Western Blot Substrate	Pierce (Thermo)	Catalogue number 80196

Continued

Continued

Reagent or resource	Source	Identifier
Chemicals, Peptides, and Recombinant Proteins		
Antigen retrieval buffer	Vector	Catalogue number H-3300
Bovine Serum Albumin (BSA) Fraction V	Calbiochem	Catalogue number 2930
Complete EDTA-free protease inhibitor	Millipore-Sigma (Roche)	Catalogue number 11836170001
Glycerol	Calbiochem	Catalogue number 4750
Glycine	JT Baker	Catalogue number 4059-02
Hoechst 33342	ThermoFisher Scientific	Catalogue number 62249
Intercept TBS Blocking Buffer	Li-Cor	Catalogue number 927-60001
Milk/Blocking solution	Bio-Rad	Catalogue number 170-6404
Normal Goat Serum (NGS)	Novex (Life Technologies)	Catalogue number PCN5000
Paraformaldehyde (16%)	Electron Microscopy Sciences	Catalogue number # 15710-S
Phosphate Buffered Saline (PBS)	Sigma	Catalogue number D5652
Poly-L-lysine	Millipore-Sigma	Catalogue number A005C
Ponceau S	Sigma	Catalogue number P3504
ProLong Gold Antifade Mountant	Thermo Fisher Scientific	Catalogue number P36934
Tris Buffered Saline (TBS)	Bio-Rad	Catalogue number 1706435
Tris-Glycine-SDS Running Buffer	Bio-Rad	Catalogue number 1610732
Triton-X100	Sigma	Catalogue number T8787
Tween-20	Fisher	Catalogue number BP337-100
Xylene	Fisher	Catalogue number X3P
Zamboni's fixative	Newcomer Supply	Catalogue number 1459A
Mouse *Ctnna3* primers	IDT	Custom: FP: 5'-GGTTACTACCCTGGTGAATTGTCC-3′, RP: 5'-CTCTTTTCGAACTTCCTGGAGTGC-3′.
Experimental Models: Organisms/Strains		
Mouse: C57BL/6-Ctnna3em1Cgot	NU Transgenic & Targeted Mutagenesis Core Facility	Genotyping via Transnetyx (real-time qPCR validation); JAX Stock No. 037394 in process
Mouse: C57BL/6J	Jackson Labs	JAX: 000664
Software and Algorithms		
FIJI/ImageJ (version: 2.1.0/1.53c)	Schneider et al., 2012	https://imagej.nih.gov/ij/
Imaris		https://imaris.oxinst.com/
Other		
Beadblaster 24	Benchmark	D2400
Beadbug Homogenizer Tubes	Sigma	Catalogue number Z763802
Sonifier 450	Branson	450
MyiQ Single Color Real-Time PCR Detection System	BioRad	Catalogue number 170-9770
Tissue Tearor	Biospec	985370-395
Li-Cor Odyssey FC Imager	Li-Cor	
Transblot Turbo	Bio-Rad	
MZ FL III Fluorescence stereomicroscope	Leica	
W1 Spinning Disk Confocal	Nikon Instruments	
Axioplan2 epifluorescence microscope	Zeiss; 20× objective (Air)	AxioCAM HR Camera with AxioVision 4.8 software

Acknowledgements
We thank Bruce Appel (University of Colorado, Denver) for the membrane-anchored eGFPcaax construct and Lynn Doglio, Eugene Wyatt and Rajesh Awatramani at Northwestern University's Transgenic Mouse Core for advice and design of the *Ctnna3*$^{GFP/+}$ reporter mouse line. We thank Robert P. Schleimer (Allergy and Immunology, Northwestern) and Bradley Undem (Johns Hopkins University) for discussions regarding vagal contributions to asthma.

Competing interests
The authors declare no competing or financial interests.

Author Contributions
Conceptualization: C.J.G.; Methodology: R.P.A., S.E.C.; Validation: A.W., E.E.R., A.S.F., S.E.C.; Formal analysis: A.W., S.E.C., C.J.G.; Investigation: A.W., E.E.R., A.S.F., S.E.C.; Writing - original draft: A.W., E.E.R., C.J.G.; Writing - review & editing: A.S.F., S.E.C., C.J.G.; Visualization: A.W., E.E.R., A.S.F.; Supervision: C.J.G.; Project administration: C.J.G.; Funding acquisition: C.J.G.

Funding
C.J.G. was supported by Northwestern University Allergy Immunology Research Program (NUAIR; T32AI083216), GM129312, HL134800, Center for Advanced Microscopy (NCI CCSG P30 CA060553; S10 RR031680; S10OD016342).Open Access funding provided by Northwestern University. Deposited in PMC for immediate release.

References

Bacchelli, E., Ceroni, F., Pinto, D., Lomartire, S., Giannandrea, M., D'adamo, P., Bonora, E., Parchi, P., Tancredi, R., Battaglia, A. et al. (2014). A CTNNA3 compound heterozygous deletion implicates a role for alphaT-catenin in susceptibility to autism spectrum disorder. *J. Neurodev. Disord.* **6**, 17. doi:10.1186/1866-1955-6-17

Bernstein, D. I., Kashon, M., Lummus, Z. L., Johnson, V. J., Fluharty, K., Gautrin, D., Malo, J. L., Cartier, A., Boulet, L. P., Sastre, J. et al. 2013). CTNNA3 (alpha-catenin) gene variants are associated with diisocyanate asthma: a replication study in a Caucasian worker population. *Toxicol. Sci.* **131**, 242-246. doi:10.1093/toxsci/kfs272

Chiarella, S. E., Rabin, E. E., Ostilla, L. A., Flozak, A. S. and Gottardi, C. J. (2018). αT-catenin: a developmentally dispensable, disease-linked member of the alpha-catenin family. *Tissue Barriers* **6**, e1463896. doi:10.1080/21688370.2018.1463896

Fannon, A. M., Sherman, D. L., Ilyina-Gragerova, G., Brophy, P. J., Friedrich, V. L., Jr. and Colman, D. R. (1995). Novel E-cadherin-mediated adhesion in peripheral nerve: Schwann cell architecture is stabilized by autotypic adherens junctions. *J. Cell Biol.* **129**, 189-202. doi:10.1083/jcb.129.1.189

Folmsbee, S. S. and Gottardi, C. J. (2017). Cardiomyocytes of the heart and pulmonary veins: novel contributors to asthma? *Am. J. Respir. Cell Mol. Biol.* **57**, 512-518. doi:10.1165/rcmb.2016-0261TR

Folmsbee, S. S., Morales-Nebreda, L., Van Hengel, J., Tyberghein, K., Van Roy, F., Budinger, G. R., Bryce, P. J. and Gottardi, C. J. (2015). The cardiac protein αT-catenin contributes to chemical-induced asthma. *Am. J. Physiol.* **308**, L253-L258. doi:10.1152/ajplung.00331.2014

Folmsbee, S. S., Budinger, G. R. S., Bryce, P. J. and Gottardi, C. J. (2016a). The cardiomyocyte protein alphaT-catenin contributes to asthma through regulating pulmonary vein inflammation. *J. Allergy Clin. Immunol.* **138**, 123-129.e2. doi:10.1016/j.jaci.2015.11.037

Folmsbee, S. S., Wilcox, D. R., Tyberghein, K., De Bleser, P., Tourtellotte, W. G., Van Hengel, J., Van Roy, F. and Gottardi, C. J. (2016b). αT-catenin in restricted brain cell types and its potential connection to autism. *J. Mol. Psychiatry* **4**, 2. doi:10.1186/s40303-016-0017-9

Franke, W. W., Borrmann, C. M., Grund, C. and Pieperhoff, S. (2006). The area composita of adhering junctions connecting heart muscle cells of vertebrates. I. Molecular definition in intercalated disks of cardiomyocytes by immunoelectron microscopy of desmosomal proteins. *Eur. J. Cell Biol.* **85**, 69-82. doi:10.1016/j.ejcb.2005.11.003

Gerber, D., Pereira, J. A., Gerber, J., Tan, G., Dimitrieva, S., Yángüez, E. and Suter, U. (2021). Transcriptional profiling of mouse peripheral nerves to the single-cell level to build a sciatic nerve ATlas (SNAT). *Elife* **10**, e58591. doi:10.7554/eLife.58591

GTEx Consortium. (2013). The genotype-tissue expression (GTEx) project. *Nat. Genet.* **45**, 580-585. doi:10.1038/ng.2653

Herrenknecht, K., Ozawa, M., Eckerskorn, C., Lottspeich, F., Lenter, M. and Kemler, R. (1991). The uvomorulin-anchorage protein alpha catenin is a vinculin homologue. *Proc. Natl. Acad. Sci. USA* **88**, 9156-9160. doi:10.1073/pnas.88.20.9156

Hines, J. H., Ravanelli, A. M., Schwindt, R., Scott, E. K. and Appel, B. (2015). Neuronal activity biases axon selection for myelination in vivo. *Nat. Neurosci.* **18**, 683-689. doi:10.1038/nn.3992

Hirano, S., Kimoto, N., Shimoyama, Y., Hirohashi, S. and Takeichi, M. (1992). Identification of a neural alpha-catenin as a key regulator of cadherin function and multicellular organization. *Cell* **70**, 293-301. doi:10.1016/0092-8674(92)90103-J

Janssens, B., Goossens, S., Staes, K., Gilbert, B., Van Hengel, J., Colpaert, C., Bruyneel, E., Mareel, M. and Van Roy, F. (2001). αT-catenin: a novel tissue-specific β-catenin-binding protein mediating strong cell-cell adhesion. *J. Cell Sci.* **114**, 3177-3188. doi:10.1242/jcs.114.17.3177

Janssens, B., Mohapatra, B., Vatta, M., Goossens, S., Vanpoucke, G., Kools, P., Montoye, T., Van Hengel, J., Bowles, N. E., Van Roy, F. et al. (2003). Assessment of the CTNNA3 gene encoding human αT-catenin regarding its involvement in dilated cardiomyopathy. *Hum. Genet.* **112**, 227-236. doi:10.1007/s00439-002-0857-5

Kim, S. H., Cho, B. Y., Park, C. S., Shin, E. S., Cho, E. Y., Yang, E. M., Kim, C. W., Hong, C. S., Lee, J. E. and Park, H. S. (2009). Alpha-T-catenin (CTNNA3) gene was identified as a risk variant for toluene diisocyanate-induced asthma by genome-wide association analysis. *Clin. Exp. Allergy* **39**, 203-212. doi:10.1111/j.1365-2222.2008.03117.x

Lewis, M. J., Short, A. L. and Lewis, K. E. (2006). Autonomic nervous system control of the cardiovascular and respiratory systems in asthma. *Respir. Med.* **100**, 1688-1705. doi:10.1016/j.rmed.2006.01.019

Li, J. and Radice, G. L. (2010). A new perspective on intercalated disc organization: implications for heart disease. *Dermatol. Res. Pract.* **2010**, 207835. doi:10.1155/2010/207835

Li, J., Goossens, S., Van Hengel, J., Gao, E., Cheng, L., Tyberghein, K., Shang, X., De Rycke, R., Van Roy, F. and Radice, G. L. (2012). Loss of αT-catenin alters the hybrid adhering junctions in the heart and leads to dilated cardiomyopathy and ventricular arrhythmia following acute ischemia. *J. Cell Sci.* **125**, 1058-1067. doi:10.1242/jcs.098640

Li, J., Fung, I., Glessner, J. T., Pandey, R., Wei, Z., Bakay, M., Mentch, F. D., Pellegrino, R., Wang, T., Kim, C. et al. (2015). Copy number variations in CTNNA3 and RBFOX1 associate with pediatric food allergy. *J. Immunol.* **195**, 1599-1607. doi:10.4049/jimmunol.1402310

Li, Y., Merkel, C. D., Zeng, X., Heier, J. A., Cantrell, P. S., Sun, M., Stolz, D. B., Watkins, S. C., Yates, N. A. and Kwiatkowski, A. V. (2019). The N-cadherin interactome in primary cardiomyocytes as defined using quantitative proximity proteomics. *J. Cell Sci.* **132**, jcs221606. doi:10.1242/jcs.221606

Lien, W. H., Klezovitch, O., Fernandez, T. E., Delrow, J. and Vasioukhin, V. (2006). alphaE-catenin controls cerebral cortical size by regulating the hedgehog signaling pathway. *Science* **311**, 1609-1612. doi:10.1126/science.1121449

Maltese, P. E., Aldanova, E., Kriuchkova, N., Averianov, A., Manara, E., Paolacci, S., Bruson, A., Miotto, R., Sartori, M., Guerri, G. et al. (2019). Putative role of Brugada syndrome genes in familial atrial fibrillation. *Eur. Rev. Med. Pharmacol. Sci.* **23**, 7582-7598. doi:10.26355/eurrev_201909_18880

Mcalexander, M. A., Gavett, S. H., Kollarik, M. and Undem, B. J. (2015). Vagotomy reverses established allergen-induced airway hyperreactivity to methacholine in the mouse. *Respir. Physiol. Neurobiol.* **212-214**, 20-24. doi:10.1016/j.resp.2015.03.007

Mcgeachie, M. J., Wu, A. C., Tse, S. M., Clemmer, G. L., Sordillo, J., Himes, B. E., Lasky-Su, J., Chase, R. P., Martinez, F. D., Weeke, P. et al. 2015). CTNNA3 and SEMA3D: promising loci for asthma exacerbation identified through multiple genome-wide association studies. *J. Allergy Clin. Immunol.* **136**, 1503-1510. doi:10.1016/j.jaci.2015.04.039

Mcgovern, A. E. and Mazzone, S. B. (2014). Neural regulation of inflammation in the airways and lungs. *Auton. Neurosci.* **182**, 95-101. doi:10.1016/j.autneu.2013.12.008

Miyashita, A., Arai, H., Asada, T., Imagawa, M., Matsubara, E., Shoji, M., Higuchi, S., Urakami, K., Kakita, A., Takahashi, H., and **Japanese Genetic Study Consortium for Alzeheimer's Disease.** et al. (2007). Genetic association of CTNNA3 with late-onset Alzheimer's disease in females. *Hum. Mol. Genet.* **16**, 2854-2869. doi:10.1093/hmg/ddm244

Norgren, R. and Smith, G. P. (1994). A method for selective section of vagal afferent or efferent axons in the rat. *Am. J. Physiol.* **267**, R1136-R1141. doi:10.1152/ajpcell.1994.267.4.C1136

O'Roak, B. J., Vives, L., Girirajan, S., Karakoc, E., Krumm, N., Coe, B. P., Levy, R., Ko, A., Lee, C., Smith, J. D. et al. (2012). Sporadic autism exomes reveal a highly interconnected protein network of de novo mutations. *Nature* **485**, 246-250. doi:10.1038/nature10989

Park, C., Falls, W., Finger, J. H., Longo-Guess, C. M. and Ackerman, S. L. (2002). Deletion in Catna2, encoding alpha N-catenin, causes cerebellar and hippocampal lamination defects and impaired startle modulation. *Nat. Genet.* **31**, 279-284. doi:10.1038/ng908

Perin, P. and Potocnik, U. (2014). Polymorphisms in recent GWA identified asthma genes CA10, SGK493, and CTNNA3 are associated with disease severity and treatment response in childhood asthma. *Immunogenetics* **66**, 143-151. doi:10.1007/s00251-013-0755-0

Schneider, C. A., Rasband, W. S. and Eliceiri, K. W. (2012). NIH Image to ImageJ: 25 years of image analysis. *Nat. Methods* **9**, 671-675. doi:10.1038/nmeth.2089

Sheikh, F., Chen, Y., Liang, X., Hirschy, A., Stenbit, A. E., Gu, Y., Dalton, N. D., Yajima, T., Lu, Y., Knowlton, K. U. et al. (2006). alpha-E-catenin inactivation disrupts the cardiomyocyte adherens junction, resulting in cardiomyopathy and susceptibility to wall rupture. *Circulation* **114**, 1046-1055. doi:10.1161/CIRCULATIONAHA.106.634469

Smith, D. I., Zhu, Y., Mcavoy, S. and Kuhn, R. (2006). Common fragile sites, extremely large genes, neural development and cancer. *Cancer Lett.* **232**, 48-57. doi:10.1016/j.canlet.2005.06.049

Teodorovich, N., Kogan, Y., Paz, O. and Swissa, M. (2016). Vagally mediated ventricular arrhythmia in Brugada syndrome. *HeartRhythm Case Rep.* **2**, 530-535. doi:10.1016/j.hrcr.2016.08.016

Torres, M., Stoykova, A., Huber, O., Chowdhury, K., Bonaldo, P., Mansouri, A., Butz, S., Kemler, R. and Gruss, P. (1997). An alpha-E-catenin gene trap mutation defines its function in preimplantation development. *Proc. Natl. Acad. Sci. USA* **94**, 901-906. doi:10.1073/pnas.94.3.901

Tricaud, N., Perrin-Tricaud, C., Bruses, J. L. and Rutishauser, U. (2005). Adherens junctions in myelinating Schwann cells stabilize Schmidt-Lanterman incisures via recruitment of p120 catenin to E-cadherin. *J. Neurosci.* **25**, 3259-3269. doi:10.1523/JNEUROSCI.5168-04.2005

Uemura, M. and Takeichi, M. (2006). Alpha N-catenin deficiency causes defects in axon migration and nuclear organization in restricted regions of the mouse brain. *Dev. Dyn.* **235**, 2559-2566. doi:10.1002/dvdy.20841

Van Hengel, J., Calore, M., Bauce, B., Dazzo, E., Mazzotti, E., De Bortoli, M., Lorenzon, A., Li Mura, I. E., Beffagna, G., Rigato, I. et al. (2013). Mutations in the area composita protein alphaT-catenin are associated with arrhythmogenic right ventricular cardiomyopathy. *Eur. Heart J.* **34**, 201-210. doi:10.1093/eurheartj/ehs373

Vasioukhin, V., Bauer, C., Degenstein, L., Wise, B. and Fuchs, E. (2001). Hyperproliferation and defects in epithelial polarity upon conditional ablation of alpha-catenin in skin. *Cell* **104**, 605-617. doi:10.1016/S0092-8674(01)00246-X

Vilarino-Guell, C., Zimprich, A., Martinelli-Boneschi, F., Herculano, B., Wang, Z., Matesanz, F., Urcelay, E., Vandenbroeck, K., Leyva, L., Gris, D. et al. (2019). Exome sequencing in multiple sclerosis families identifies 12 candidate genes and nominates biological pathways for the genesis of disease. *PLoS Genet.* **15**, e1008180. doi:10.1371/journal.pgen.1008180

Vite, A., Li, J. and Radice, G. L. (2015). New functions for alpha-catenins in health and disease: from cancer to heart regeneration. *Cell Tissue Res.* **360**, 773-783. doi:10.1007/s00441-015-2123-x

Wang, K., Zhang, H., Ma, D., Bucan, M., Glessner, J. T., Abrahams, B. S., Salyakina, D., Imielinski, M., Bradfield, J. P., Sleiman, P. M. et al. (2009). Common genetic variants on 5p14.1 associate with autism spectrum disorders. *Nature* **459**, 528-533. doi:10.1038/nature07999

Zhang, Y., Chen, K., Sloan, S. A., Bennett, M. L., Scholze, A. R., O'keeffe, S., Phatnani, H. P., Guarnieri, P., Caneda, C., Ruderisch, N. et al. (2014). An

RNA-sequencing transcriptome and splicing database of glia, neurons, and vascular cells of the cerebral cortex. *J. Neurosci.* **34**, 11929-11947. doi:10.1523/JNEUROSCI.1860-14.2014

Zhang, Y., Sloan, S. A., Clarke, L. E., Caneda, C., Plaza, C. A., Blumenthal, P. D., Vogel, H., Steinberg, G. K., Edwards, M. S., Li, G.3rd, et al. (2016). Purification and characterization of progenitor and mature human astrocytes reveals transcriptional and functional differences with mouse. *Neuron* **89**, 37-53. doi:10.1016/j.neuron.2015.11.013

Zhang, Y., Zhou, X., Dai, W., Sun, J., Lin, M., Zhang, Y. and Ding, Y. (2021). CTNNA3 genetic polymorphism may be a new genetic signal of type 2 diabetes in the Chinese Han population: a case control study. *BMC Med. Genomics* **14**, 257. doi:10.1186/s12920-021-01105-8